

## Reentrant Spin Glass Behavior in Cr-Doped Perovskite Manganite

Joonghoe Dho, W. S. Kim, and N. H. Hur\*

Center for CMR materials, Korea Research Institute of Standards and Science, Yusong P.O. Box 102,  
Taejeon, 305-600 Korea

(Received 28 December 2001; published 20 June 2002)

The magnetic and transport properties of the Cr-doped manganites  $\text{La}_{0.46}\text{Sr}_{0.54}\text{Mn}_{1-y}\text{Cr}_y\text{O}_3$  ( $0 \leq y \leq 0.08$ ) with the *A*-type antiferromagnetic structure were investigated. Upon cooling, we find multiple magnetic phase transitions, i.e., paramagnetic, ferromagnetic (FM), antiferromagnetic (AFM), and spin glass in the  $y = 0.02$  sample. The low temperature spin glass state is not a conventional spin glass with randomly oriented magnetic moments but has a reentrant character. The reentrant spin glass behavior accompanied by the anomalous multiple magnetic transitions might be due to the competing interactions between the FM phase and the *A*-type AFM matrix induced by the random Cr impurity.

DOI: 10.1103/PhysRevLett.89.027202

PACS numbers: 75.30.Vn, 75.30.Kz, 75.60.Nt

The magnetic ground state of the doped perovskite manganite  $R_{1-x}A_x\text{MnO}_3$  ( $R$  = rare-earth ion,  $A$  = alkaline-earth ion) near  $x \sim 0.5$  is very sensitive to the average radius of the  $R/A$  cations,  $\langle r_A \rangle$  [1–4]. It has been known that ground states of  $\text{La}_{0.5}\text{Ca}_{0.5}\text{MnO}_3$  and  $\text{Nd}_{0.5}\text{Ca}_{0.5}\text{MnO}_3$  with relatively small  $\langle r_A \rangle$  are the CE-type antiferromagnetic (AFM) structure [3,5], whereas,  $\text{Pr}_{0.5}\text{Sr}_{0.5}\text{MnO}_3$  and  $\text{La}_{0.46}\text{Sr}_{0.54}\text{MnO}_3$  with large  $\langle r_A \rangle$  have the *A*-type AFM ground state. This can be understood as a result of the enhanced bandwidth ( $W$ ) for the itinerant  $e_g$  electron in the *A*-type compounds [3,4]. In addition, the stability of the AFM ground state also depends on the impurity doping onto the Mn site [5–11]. For instance, the Cr doping significantly suppresses the AFM state regardless of its nature and makes the system ferromagnetic (FM). In the Cr-doped CE-type AFM compound, Kimura *et al.* found a very unique relaxor FM behavior with the diffuse phase transition and the history-dependent growth of FM clusters, which is mainly due to the quenched random field originating from the Cr impurity [5]. On the other hand, any extraordinary phenomenon has not been observed yet in the *A*-type AFM manganite although it also changes from AFM to FM by the Cr doping.

In the course of studying magnetic and transport properties of the Cr-doped manganites  $\text{La}_{0.46}\text{Sr}_{0.54}\text{Mn}_{1-y}\text{Cr}_y\text{O}_3$  ( $0 \leq y \leq 0.08$ ) with the *A*-type spin structure, we have observed anomalous multiple magnetic transitions, namely, paramagnetic (PM), FM, AFM, and spin glass in  $y = 0.02$ . Furthermore, the low temperature spin glass state is not a typical spin glass phase observed in a variety of disordered magnetic systems but a reentrant spin glass (RSG) [12–14]. This is the first example to show the RSG phenomenon associated with both FM and AFM transition. The RSG system known thus far has either long-range FM or AFM ordering above the spin glass transition temperature [15–21]. Upon cooling, the ordered state is frustrated with increasing the random FM or AFM interactions and as a result undergoes the RSG transition. The RSG phenomenon resulting from the frustration of the *A*-type AFM manganite is comparable with a relaxor

ferromagnet induced by the collapse of the charge ordered CE-type AFM state in  $\text{Nd}_{0.5}\text{Ca}_{0.5}\text{Mn}_{0.98}\text{Cr}_{0.02}\text{O}_3$  [5]. An important feature is that the subtle difference in the spin structure leads to drastic change in physical property. It is thus the main objective of this Letter to report that the RSG behavior relevant to both FM and AFM transitions indeed exists in the *A*-type AFM manganite. In this work, we have investigated the magnetic behavior of the Cr-doped manganites in terms of the dc and ac magnetic susceptibility measurements.

Polycrystalline samples of  $\text{La}_{0.46}\text{Sr}_{0.54}\text{Mn}_{1-y}\text{Cr}_y\text{O}_3$  ( $0 \leq y \leq 0.08$ ) were prepared by the conventional solid state reaction method [14]. Stoichiometric mixtures of  $\text{La}_2\text{O}_3$ ,  $\text{SrCO}_3$ ,  $\text{Cr}_2\text{O}_3$ , and  $\text{MnO}_2$  were calcined twice at 1000 °C for 24 h in air, which were then ground and pressed into pellets. The samples were sintered at 1550 °C for 72 h in air with a couple of intermediate grindings, which were annealed at 1400 °C for 48 h under the  $\text{O}_2$  atmosphere to saturate the oxygen site. Powder x-ray diffraction patterns of all the Cr-doped samples revealed that they have a single perovskite-type phase with the tetragonal symmetry  $I4/mcm$  at room temperature. Magnetic and transport data were collected on a superconducting quantum interference device magnetometer and a physical property measurement system. The ac magnetic susceptibility was measured in the frequency range of 10–10 000 Hz. For the field-dependent magnetization measurement, the field was swept from +1 to –1 T in about 1 h. Electrical resistivity measurements were carried out using a standard four-probe method with the connections made with silver paint.

Magnetization data of  $\text{La}_{0.46}\text{Sr}_{0.54}\text{Mn}_{1-y}\text{Cr}_y\text{O}_3$  ( $0 \leq y \leq 0.08$ ) as a function of temperature collected at 50 G are shown in Fig. 1. For the  $y = 0.00$  sample the  $M(T)$  curve displays two sharp PM-to-FM and FM-to-AFM transitions at 272 K and 190 K, respectively. With increasing the Cr content the FM moment is newly evolved at the expense of the AFM component. The AFM transition almost completely disappears for  $y = 0.08$ , clearly showing that the Cr impurity changes the magnetic ground state from

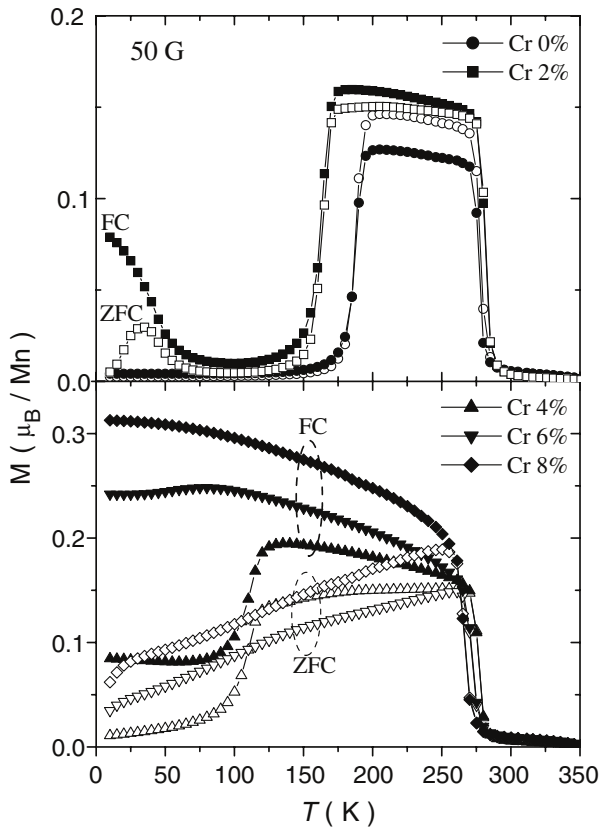


FIG. 1. Magnetization as a function of temperature for  $\text{La}_{0.46}\text{Sr}_{0.54}\text{Mn}_{1-y}\text{Cr}_y\text{O}_3$  ( $0 \leq y \leq 0.08$ ) measured in 50 G under the field-cooled (FC) and zero-field-cooled (ZFC) conditions that are denoted as the filled and open symbols, respectively.

AFM to FM. This can be attributed to the increase of the FM exchange interaction between  $\text{Mn}^{3+}$  and  $\text{Cr}^{3+}$  ions [22,23]. The overall features are somewhat similar to that found in the Cr-doped manganites with the charge ordered CE-type AFM structure [5,7,9]. In the FM state, a large splitting between the FC and ZFC curves is ascribed to the pinning of the domain wall. However, their magnetic behaviors are quite different in the low Cr-doped region. As can be clearly seen in the top panel of Fig. 1, an additional spin-glass-like transition appears in the  $y = 0.02$  sample, which is evidenced by a cusp in the ZFC curve at 40 K and a distinctive separation of the FC and ZFC curves. This feature is in marked contrast to that found in the CE-type manganite. It is thus important to further investigate the RSG behavior observed in the  $y = 0.02$  sample and to compare it with the relaxor ferromagnet in the CE-type manganite [5]. Hereafter, we mainly discuss the physical properties of the  $y = 0.02$  compound.

Figure 2 shows the temperature-dependent ac magnetic susceptibility for the  $y = 0.02$  sample at various frequencies. The measurements were performed at an ac field of 10 G after ZFC. Upon cooling from room temperature the in-phase  $\chi'(w, T)$  and out-of-phase  $\chi''(w, T)$  susceptibility curves display abrupt upturns about 280 K, exhibiting a PM-to-FM transition. The sharp drop in

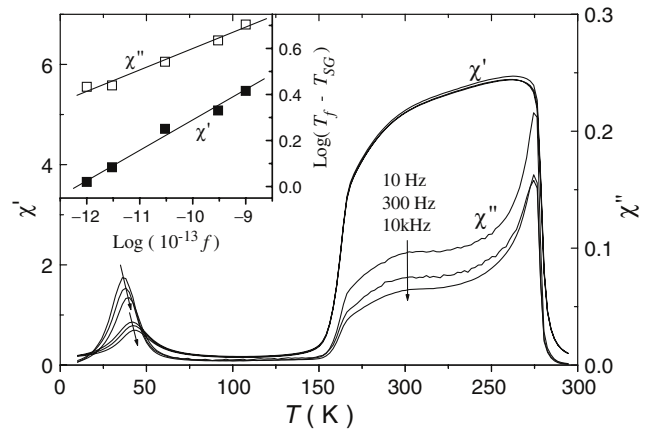


FIG. 2. The temperature dependence of the ac magnetic susceptibility for  $\text{La}_{0.46}\text{Sr}_{0.54}\text{Mn}_{0.98}\text{Cr}_{0.02}\text{O}_3$  at various frequencies. All data were collected at an ac field of 10 G upon warming in the ZFC conditions. The inset shows the best fits to the  $\chi'(w, T)$  and  $\chi''(w, T)$  data to a function of the form  $\tau/\tau_0 = [(T_f - T_{SG})/T_{SG}]^{-zv}$  with  $\tau_0 = 10^{-13}$  s.

both curves below 170 K is associated with a FM-to-AFM transition. Upon further decreasing the temperature, the  $\chi'(w, T)$  and  $\chi''(w, T)$  curves display a cusp about 40 K and 35 K, respectively. Moreover, the peak temperature of the cusp shifts towards higher temperature with increasing frequency. These features are reminiscent of a frustration of the long-range AFM state, i.e., commonly called a RSG state. A similar RSG phenomenon is observed in either a FM-based alloy like AuFe or an AFM-based compound like  $\text{Fe}_x\text{Mg}_{1-x}\text{TiO}_3$  [16–21]. With decreasing temperature the known RSG systems undergo a sequential magnetic transition of either PM-FM-RSG or PM-AFM-RSG. Unlike this, the important and distinctive feature of the RSG behavior observed in the Cr-doped manganite is that it originates from anomalous multiple magnetic transitions, namely, PM-FM-AFM-RSG transitions.

As given in Fig. 2, the maximum positions of  $\chi'(w, T)$  and  $\chi''(w, T)$  near 40 K are influenced by the frequency change. The frequency-dependent data turn out to be well described by conventional critical slowing down [16,20,24,25]:

$$\frac{\tau}{\tau_0} = \left[ \frac{(T_f - T_{SG})}{T_{SG}} \right]^{-zv} \quad (1)$$

Here,  $T_{SG}$  is the spin glass transition temperature and  $T_f$  is the frequency-dependent freezing temperature at which the maximum relaxation time  $\tau$  of the system corresponds to the measured frequency. The inset of Fig. 2 presents the best fits to the data in the 10–10 000 Hz range, indicating that the spin glass state can be well described by the slowing down model. When  $\tau_0$  is  $10^{-13}$  s typically taken in the spin glass system,  $T_{SG}$  and  $zv$  for  $\chi'(w, T)$  are 40.8 K and 7.6, respectively [25], whereas, the best fit for  $\chi''(w, T)$  yields  $T_{SG} = 34.1$  K and  $zv = 10.7$ . Although the  $T_{SG}$

and  $z\nu$  values of  $\chi'(w, T)$  and  $\chi''(w, T)$  are slightly different, their magnitudes are within the realm of conventional spin glass phase.

To further investigate the RSG behavior, we have measured the long-time relaxation of the magnetization. Figure 3 shows the magnetization and normalized magnetization  $M(t)/M(0)$  curves for the  $y = 0.02$  sample as a function of time, where the ZFC magnetization data were collected at 20 and 210 K. The magnetization at 210 K, which is in the FM state, reaches to about its saturated value upon applying field. At 20 K, on the other hand, there is a continuous increase in the magnetization even after  $10^4$  s, in which about 50% of the normalized magnetization is varied. This long-time relaxation behavior in the low temperature region is consistent with the RSG state [12,13,16]. Accordingly, the RSG state is evident in the  $y = 0.02$  sample.

In the inset of Fig. 4, we present the selected ZFC magnetization  $M(H)$  curves for the  $y = 0.02$  sample as a function of magnetic field measured at various temperatures. Both remanent magnetization  $M_R$  and coercive field  $H_C$  data obtained from the  $M(H)$  curves are almost negligible in the FM region but fairly large in the RSG state, which are given in Fig. 4. The  $M_R$  value is small above  $T_{SG}$  but suddenly increases below  $T_{SG}$ . At the same time, below  $T_{SG}$  the magnitude of  $H_C$  abruptly increases with lowering temperature. These increases of  $M_R$  and  $H_C$  with decreasing temperature are in accordance with that observed in a conventional spin glass system [15,26,27]. It is well known that in ordinary FM materials the coercive field is due to the blocking of the domain wall motion. This concept might extend to the  $y = 0.02$  system. In the RSG state, however, the  $H_C$  value is much larger than that in the FM state. As a result, the same scenario is not appropriate to explain such a large coercive field. We thus propose that

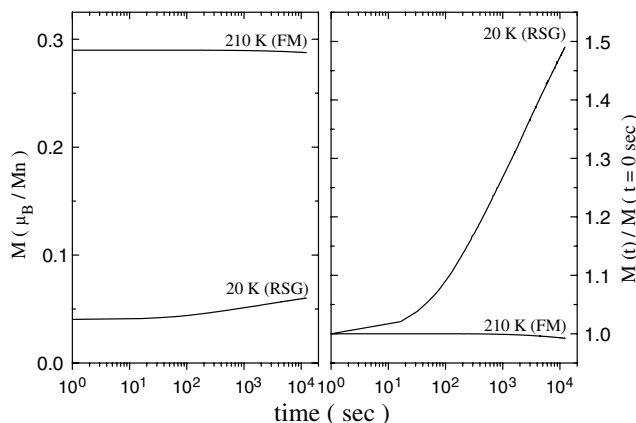


FIG. 3. The time dependence of the magnetization and normalized magnetization  $M(t)/M(0)$  curves for  $\text{La}_{0.46}\text{Sr}_{0.54}\text{Mn}_{0.98}\text{Cr}_{0.02}\text{O}_3$  at 20 and 210 K. The sample was cooled down to the measured temperature without applying magnetic field. The magnetization data were collected immediately after setting the field to 100 G.

the blocking mechanism in the RSG state originates from the frustration of the AFM phase induced by the random distribution of Cr impurities on the Mn-site [15,27].

Based on the magnetic data described above, we construct a generalized phase diagram of the Cr-doped compounds  $\text{La}_{0.46}\text{Sr}_{0.54}\text{Mn}_{1-y}\text{Cr}_y\text{O}_3$  ( $0 \leq y \leq 0.08$ ) shown in Fig. 5. In this phase diagram there is an apparent RSG state that occurs in the low Cr-doped samples. With decreasing temperature the system undergoes multiple transitions from PM to RSG via FM and AFM phases. When the Cr concentration increases, the FM phase gradually overwhelms the AFM ground state. Similar connection between impurity concentration and spin glass has also been found in other conventional spin glass systems such as  $(\text{Fe}_x\text{Ni}_{1-x})_{75}\text{P}_{16}\text{B}_6\text{Al}_3$  and  $\text{Fe}_x\text{Mg}_{1-x}\text{TiO}_3$  [16,18]. We thus conjecture that the RSG state in the Cr-doped manganite can be explained by the random-field approach suggested by Aeppli *et al.* [28]. In the Cr-doped sample the random field is induced by the interaction between the Mn ion and the randomly distributed Cr impurity.

The RSG state via multiple magnetic transitions in the Cr-doped manganite with the A-type spin structure appears to be comparable with the relaxor ferromagnet in the CE-type AFM manganite  $\text{Nd}_{0.5}\text{Ca}_{0.5}\text{Mn}_{0.98}\text{Cr}_{0.02}\text{O}_3$  [5]. In the latter the quenched random field originating from the Cr impurity is responsible for the relaxor FM behavior, in which the fraction of FM microembryos increases in the CE-type AFM insulating matrix by increasing the Cr concentration or by applying the annealing field. On the other hand, in the A-type AFM manganite the randomly distributed Cr impurity that induces a competing magnetic interaction between the FM and AFM states is the most likely cause of the RSG state. One common feature is that both phenomena are ascribed to the frustration of a long-range AFM spin ordering induced by the Cr impurity. However, their resulting properties are quite different and highly relevant to the magnetic ground states, namely, the

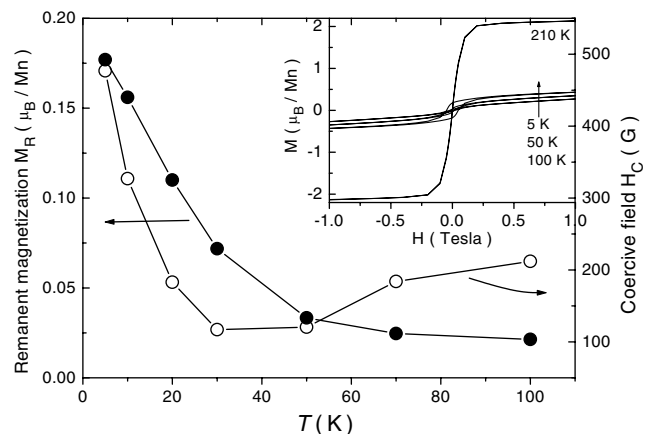


FIG. 4. The temperature dependence of remanent magnetization  $M_R$  and coercive field  $H_C$  for  $\text{La}_{0.46}\text{Sr}_{0.54}\text{Mn}_{0.98}\text{Cr}_{0.02}\text{O}_3$ . The inset shows the magnetic field dependence of the magnetization  $M(H)$  at selected temperatures.

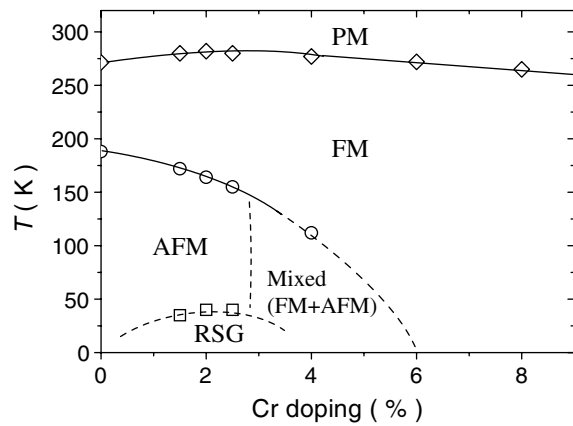


FIG. 5. Phase diagram of temperature versus Cr content ( $x$ ) for the Cr-doped manganites  $\text{La}_{0.46}\text{Sr}_{0.54}\text{Mn}_{1-y}\text{Cr}_y\text{O}_3$ . PM, FM, AFM, and RSG represent paramagnetic, ferromagnetic, antiferromagnetic, and reentrant spin glass, respectively.

charge ordered CE-type and  $d_{x^2-y^2}$  orbital ordered A-type AFM states.

As discussed above, the AFM manganite with small  $W$  displays the CE-type AFM spin and  $d_{3x^2-r^2}/d_{3y^2-r^2}$  orbital ordering, accompanied by a large lattice distortion along the three axes [3,5]. The Cr doping into the Mn site induces a short-range FM phase with mobile charge carriers in the insulating AFM matrix. An important feature is that the induced carriers tend to be confined only in the short-range FM domains due to three-dimensional nature of both the AFM background and the large lattice distortion. Theoretical study, in that charge carriers are likely to be localized when the Jahn-Teller distortion is large in the AFM manganite, supports this conjecture [29]. Accordingly, the relaxor ferromagnet behavior can be realized in the CE-type AFM matrix due to the localized FM microembryos. On the other hand, in the A-type AFM compound with the enhanced bandwidth the induced mobile charge carriers freely move within the FM layers because its spin structure has a two-dimensional nature and lattice distortion is not severe [3,30]. Therefore, the FM phases induced by the Cr doping prefer to diffuse widely in the AFM matrix rather than localize. The competing interaction between the diffused FM phase and the host AFM state eventually results in the spin glass state in the A-type AFM manganite.

In conclusion, we have revealed that the RSG state accompanied by anomalous multiple magnetic transitions indeed exists in the low Cr-doped AFM manganites with the

A-type spin structure. The resulting RSG state is mainly ascribed to the competing interaction between the FM and AFM phases. We have also found that the effect of Cr doping on the AFM manganite is heavily dependent upon the magnetic ground state. It brings the RSG state in the A-type AFM manganite, but leads to exhibit the relaxor ferromagnet behavior in the CE-type AFM compound.

This work was supported by the Creative Research Initiative Program in Korea.

\*Corresponding author.

Electronic address: nhhur@kriss.re.kr

- [1] E. O. Wollan *et al.*, Phys. Rev. **100**, 545 (1955).
- [2] J. M. D. Coey *et al.*, Adv. Phys. **48**, 167 (1999).
- [3] H. Kawano *et al.*, Phys. Rev. Lett. **78**, 4253 (1997); H. Kawano *et al.*, Physica (Amsterdam) **241B**, 289 (1998).
- [4] T. Akimoto *et al.*, Phys. Rev. B **57**, R5594 (1998).
- [5] T. Kimura *et al.*, Phys. Rev. Lett. **83**, 3940 (1999); Phys. Rev. B **62**, 15 021 (2000).
- [6] A. Maignan *et al.*, J. Appl. Phys. **89**, 500 (2001).
- [7] R. Li *et al.*, J. Appl. Phys. **88**, 5924 (2000).
- [8] R. Mahendiran *et al.*, Phys. Rev. B **64**, 064424 (2001).
- [9] Y. Moritomo *et al.*, Phys. Rev. B **60**, 9220 (1999).
- [10] B. Raveau *et al.*, J. Solid State Chem. **130**, 162 (1997).
- [11] C. Martin *et al.*, J. Magn. Magn. Mater. **202**, 11 (1999).
- [12] R. Mathieu *et al.*, Phys. Rev. B **63**, 092401 (2001).
- [13] D. N. H. Nam *et al.*, Phys. Rev. B **62**, 8989 (2000).
- [14] J. Dho *et al.*, Phys. Rev. Lett. **87**, 187201 (2001); Phys. Rev. B **65**, 024404 (2002).
- [15] I. A. Campbell *et al.*, Phys. Rev. Lett. **50**, 1615 (1983).
- [16] K. Jonason *et al.*, Phys. Rev. Lett. **77**, 2562 (1996).
- [17] I. Mirebeau *et al.*, Phys. Rev. B **41**, 11 405 (1990).
- [18] A. Ito *et al.*, Solid State Commun. **66**, 475 (1988).
- [19] A. Tobo *et al.*, J. Phys. Soc. Jpn. **67**, 297 (1998).
- [20] J. Mattsson *et al.*, Phys. Rev. Lett. **74**, 4305 (1995).
- [21] S. H. Chun *et al.*, J. Appl. Phys. **90**, 6307 (2001).
- [22] R. Ganguly *et al.*, Physica (Amsterdam) **275B**, 308 (2000).
- [23] R. Gundakaram *et al.*, J. Solid State Chem. **127**, 354 (1996).
- [24] P. C. Hohenberg *et al.*, Rev. Mod. Phys. **49**, 435 (1977).
- [25] J. A. Mydosh, *Spin Glasses* (Taylor & Francis, London, 1993).
- [26] K. Binder *et al.*, Rev. Mod. Phys. **58**, 801 (1986).
- [27] S. Mukherjee *et al.*, Phys. Rev. B **54**, 9267 (1996).
- [28] G. Aeppli *et al.*, Phys. Rev. B **28**, 5160 (1983); **29**, 2589 (1984).
- [29] S. Yunoki *et al.*, Phys. Rev. Lett. **81**, 5612 (1998).
- [30] A. Llobet *et al.*, Phys. Rev. B **60**, R9889 (1999).